



ARTICLE

A Simple Clear Technique in Observing Vascular Development of Grape Ovary

Teng Fei¹, Youmei Li¹, Bo Li² and Zhaosen Xie^{1,*}

¹College of Horticulture and Garden, Yangzhou University, Yangzhou, 225009, China

²Shandong Academy of Grape, Shandong Academy of Agricultural Sciences, Jinan, 250199, China

*Corresponding Author: Zhaosen Xie. Email: xiezhaosen@yzu.edu.cn

Received: 05 December 2022 Accepted: 27 March 2023 Published: 31 May 2023

ABSTRACT

The vascular system of the grapevine (*Vitis vinifera* L.) flower is a channel for transporting water and nutrients to the ovary. It plays an important role in the development of the ovary and fertilization through pollination. However, the vascular bundles in the flower are so tiny that they are difficult to sample and observe by traditional slicing techniques. In this study, 'Summer Black' grape flowers were selected as the test materials, and the tissue samples were treated by the optical clearing technique. After simple compaction, the structure and development of the vasculature were observed by common microscopy, fluorescence microscopy and laser confocal microscopy. The results showed that the transparency effects of 3% NaOH and a saturated trichloroacetaldehyde composite agreed well with the observations of the vascular structure and the developmental process of the flower in different periods. Moreover, the samples after optical clearing could be reconstructed in 3D, which helped us know more about its development and function. According to these observations, the vasculature of the 'Summer Black' flower can be divided into ovule vascular bundles, peripheral vascular bundles and central vascular bundles. The peripheral vascular bundles were composed of the first-order vascular bundles and the inferior vascular bundles which branched from the superior vascular bundles. These bundles branched in different directions with no discernible pattern. The two different branching methods were as follows. First, the inferior vascular bundle was directly connected to a superior vascular bundle. Secondly, some of the superior vascular bundles bent in different ways, forming the inferior vascular bundle connecting the superior vascular bundles by a metamorphosed vessel with a triangular shape. In a comparison of the developmental changes in various periods, the growth of vascular bundles at each period was directly proportional to the growth of the flower. Laser confocal scanning was used to explore the three-dimensional morphology of the peripheral vascular bundle and showed that the peripheral vascular bundle of grapes was not completely parallel to the flower's epidermal cells. As a result, the optical clearing technique was convenient and authentic compared with the traditional slicing operation for tiny flower organs. With these advantages according to the observations, this study provides a feasible technique and useful information for the study of vascular bundle development in grape flower organs.

KEYWORDS

Vitaceae; microscopy; xylem



Nomenclature

FVB	First order vascular bundle
IVB	Inferior order vascular bundle
PVB	Peripheral vascular bundle
OVB	Ovary vascular bundle
CVB	Central vascular bundle
Dm	Diameter of the first order bundle
Df	Distance from peripheral vascular bundle to the epidemic cell
Mv	Metamorphic vessel

1 Introduction

As an economic fruit plant widely planted over one million by FAO in the world, the fruit of grapevine (*Vitis vinifera* L.) is an important economic product [1,2]. The grape is a true fruit and develops from the flower ovary. Insufficient nutrient supply during the flowering period of grapes can lead to low fruit setting, and directly affects the yield and quality of the crop [3]. Unlike the increased fruit quality caused by water deficiency at the fruiting stage, the grape flower is a weak sink from the 50% bloom stage to fruit setting. Slight water stress will lead to flower abortion [4] because there is a strong nutritional competition between grape branches and flowers [5]. The vasculature supplies nutrients to the flower organs. In research into grape, it has been considered that the cross-sectional area of vessels affects their transportation ability and the size of the fruit [6,7]. There have also been some studies showing that the thickening and stretching of flower vessels can improve the quality of fruit in grape [8]. In a study of the hydraulic isolation of xylem in vascular bundles of the fruit, Chatelet proposed that the initial stage of the fruit's vasculature should be studied systematically [9]. Studying the development of floral organs, especially the vascular development of floral organs, is of great significance for production and scientific research.

To study the development of grape flowers, previous studies observed the floral organs in different periods by scanning electron microscopy and paraffin sections and summarized the changes in floral organ size and external morphology in different periods [10,11]. However, studies on the vascular structure and development of floral organs are rare. Anatomical research on the vascular structure of grape mainly focused on the development and functional changes [9,12,13]. Dye injection and maceration have been used most often for studying the vascular development and changes in function in grape. In recent years, Zeyu observed and studied the vascular arrangement of fruit by micro-CT [14], and Knife used laser scanning technology to reconstruct the vasculature of the fruit of grape in three dimensions [15]. However, compared with the fruits, the vasculature of flower organs is so tiny that the dye injection is difficult to operate while the vascular structure is easily destroyed in the process of isolation. It is difficult to apply CT scanning and 3D imaging [16] because the flower of 'Summer Black' is not as transparent as the fruit.

Many optical clearing agents, however, can remove the self-fluorescence properties of the sample during the process of removing the pigment, which can interfere with observations of the fluorescence [17]. In order to study the vascular development of flowers, selected optical clearing agents were used on the tissues in this experiment. After the transparency treatment, the ovary of 'Summer Black' grape flowers was observed by brightfield, fluorescence and three-dimensional imaging. The 3% NaOH solution and chloral hydrate used in this experiment as optical clearing agents are routine laboratory reagents and did not affect the observations of fluorescence. The three-dimensional structure of the peripheral vascular bundle of grape flower ovary was

observed and reconstructed successfully by fluorescence microscopy and confocal three-dimensional imaging technology. At the same time, paraffin sections were used to observe the vasculature of ‘Summer Black’ flowers. The advantages and disadvantages of both experimental methods were compared. This study provided a theoretical and technical basis for studying the vascular development of the floral organs of grape and the advantages of pruning at flowering stage to regulate fruit quality.

In this study, an optical clearing technique was selected to deal with samples. As a technique which can be used to observe cell tissues systematically and completely, the optical clearing technique has become an important research technique in the fields of biology and medicine. With this technology, the sample is made transparent with optical clearing agents, which reduce the light refractive index and reflectivity of the sample, allowing the internal structure of the sample to be observed without damaging the sample. This way, fluorescence microscopy and confocal laser scanning can be better used to take three-dimensional images and analyze the three-dimensional tissues. The optical clearing method can be used to quickly observe the internal structure and development process of tissues and is a quick method for learning more about the development and function of the vasculature when the berries are at the start of development.

2 Materials and Methods

2.1 Plant Materials

Flowers were obtained from 3-year-old ‘Summer Black’ grapevines planted with the same cultivation and management conditions at Jin Niushan Experimental Station at Shang Dong Institute of Pomology. The flowers were divided into six stages: visible clusters, cluster separation, floral bud separation, 50% bloom (the onset of flowering), 100% bloom (end of flowering) and fruit set [18]. From 9:00 a.m. to 10:00 a.m. in May–June 2021, the flowers were collected and brought back to the laboratory, and the pistils and stamens were peeled off instantly. Three clusters of grape spikes with the same growth potential were selected in each period as three biological repetitions.

2.2 Chemicals

The following chemicals were used in this study: sodium hydroxide (CAS No. 1310-73-2, Macklin), chloral hydrate (CAS No. 75-87-6, Sigma), pectinase (CAS No. 9032-75-1, Macklin), cellulase (CAS No. 9012-54-8, Macklin), toluidine blue (CAS No. 6586-04-5, Macklin).

2.3 Experimental Methods

2.3.1 Clear Samples and Observation

Grape flowers with similar sizes were selected from different developmental periods, and were placed in a 3% NaOH solution. After soaking for 2 h, the flower pigments faded out of the ovary and turned black. After 3 days, the pigment faded completely. After 5 days, the ovary of flower was clear, with the solution being changed continuously during this stage. Grape flowers were taken out of the solution, washed with deionized water for 2–3 times, placed in a saturated chloral hydrate solution and left to stand for 2–4 h until the flower organ was completely transparent [19].

The specific method used for staining the grape flowers was as follows. Two or three drops of a 1% toluidine blue stain solution were taken with a rubber-tipped dropper and added to an aqueous solution containing the transparent flower. The flowers were stained for about 5 min, taken out gently with tweezers, and placed in a glycerin solution for preservation. The stained grape flower was gently taken out and placed on the slide. The ovaries were cut longitudinally by a sharp blade in the direction of the style, with the section facing down. The placement position of the flowers was gently adjusted with tweezers, a small amount of glycerin was dripped onto the flower with a glass rod, and the cover glass

was gently pressed horizontally onto the slide until the flower organ was flat. The experimental process is shown in Fig. 1.

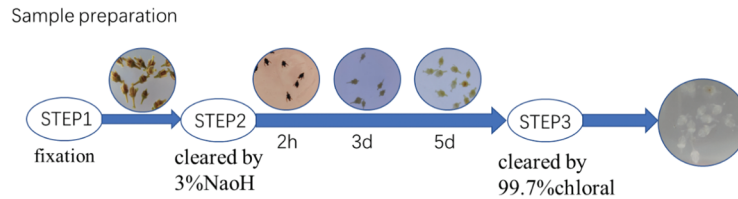


Figure 1: Transparent effect of ‘Summer Black’ flower ovary

2.3.2 Paraffin Section

The samples for paraffin sectioning were treated according to [20]. The samples (six stages) were fixed with FAA (70% ethanol:acetic acid:formalin, 18:1:1, v/v/v). Then the samples were dehydrated in increasing concentrations of ethanol (50%, 75%, 90% and 100%) for 30 min in each ethanol solution. Afterwards, the samples were embedded in paraffin and 10 μm sections were prepared using a rotary microtome (RM2125 RTS, Leica, Heidelberg, Germany). Finally, the sections were mounted on a glass slide and stained with 1% safranin and 1% fast green. The staining times were 5 min for safranin and 20 s for fast green.

2.3.3 Confocal Laser Scanning

The samples which had been treated as described in Section 2.3.1 were placed on the stage of the imaging system of the laser confocal microscope (LSM 880NLO, Carl Zeiss). The samples were observed, and pictures were taken by layer scanning. The parameters were set as a linear scanning speed of 13 frames per second at 512×512 . The wavelength of blue light excited by WGA-AF488 was 488 nm, and the wavelength of the emitted light was 510 nm.

Sixty-four pictures of each sample at different heights were taken for 3D reconstruction. Zen Blue (Carl Zeiss, Germany) was used as a stacking frame for the 3D reconstruction. Brightfield images were taken after stacking.

2.3.4 Measurement and Statistics

The size and number of vessels were counted by Image J (on GitHub), and the mean value and significance were calculated by SPSS 26 (IBM, US). Measurement and statistics for the 3D images were collected by Zen Blue (Carl Zeiss, Germany).

3 Results and Analysis

3.1 Transparency and Observations

In this experiment, 3% NaOH and chloral hydrate were used as optical clearing agents. When the pigment was precipitated with NaOH, the area of the stigma turned black at first and then the color became completely white. The ovary was then precipitated. Using the NaOH solution alone could successfully precipitate the pigment of flower organs, but the flower organs were not completely transparent, requiring further treatment with chloral hydrate (Fig. 1). The vasculature of the stained flower ovary could be clearly seen under fluorescence and by brightfield imaging after the entire treatment. The confocal scanning technique could reconstruct the three-dimensional structure of the vasculature (Fig. 2).

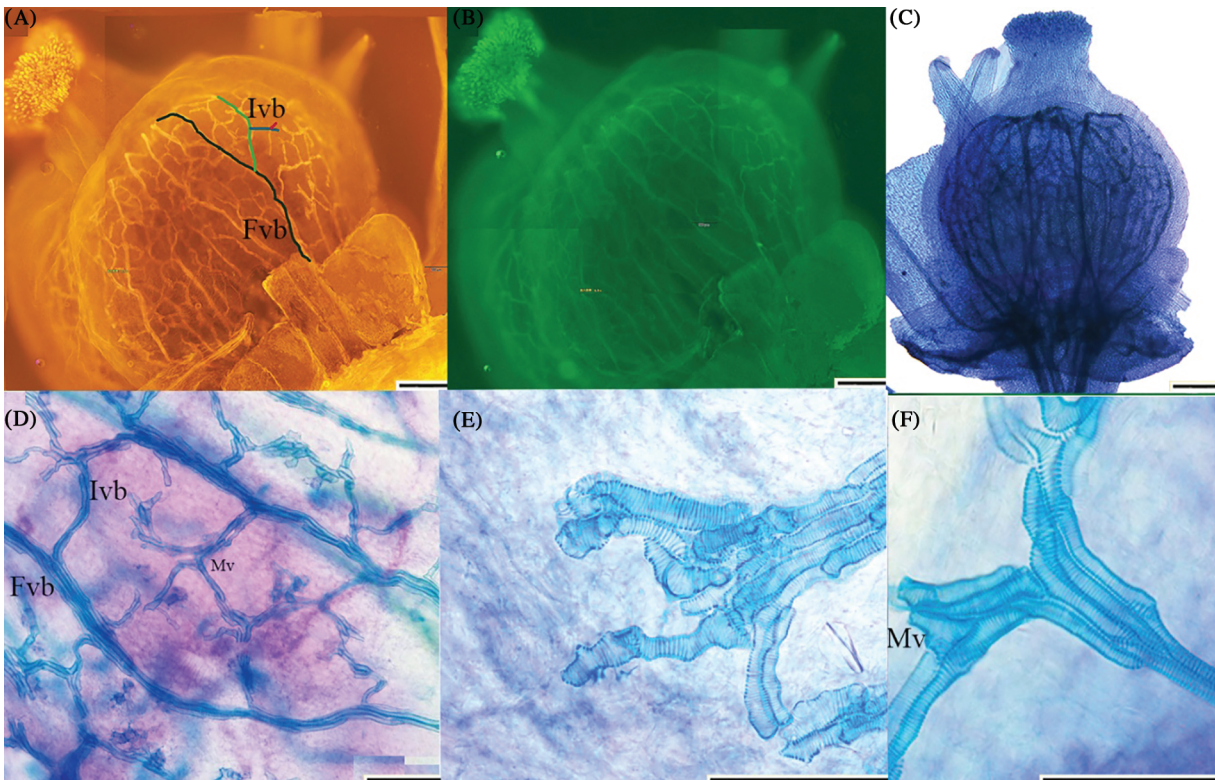


Figure 2: Observation effect of ovary of 'Summer Black' flower. (A) red fluorescent organ vasculature of 'Summer Black' flower 10 times; First order vascular bundle and inferior vascular bundle could be observed clearly; FVB First order vascular bundle ; IVB Inferior order vascular bundle; (B) green fluorescent organ vasculature of 'Summer Black' ovary 10 times; (C, D) under bright field 10 times 20 times. The arrangement and branches of vascular bundle could be observed clearly; (E, F) 40 times can clearly see the structure of the vessels; (E) showed terminal vessels in vascular bundles; (F) showed the connection of the superior vascular bundle to inferior vascular bundle. Mv Metamorphic vessel. The pattern of the secondary cell wall was almost all helical (scale 200 μm)

3.2 Ovary Morphology and Development of 'Summer Black' Flowers

The morphology and development of 'Summer Black' flower ovaries showed certain changes from the visible cluster stage to the fruit setting stage. The diameter of the flower ovary in the visible cluster stage was less than 0.5 mm, and the ovary was completely wrapped by a flower cap. The diameter of the ovary at the cluster separation stage exceeded 0.7 mm, and the ovary was still wrapped by a flower cap. The diameter of the flower at the floral bud separation stage was twice as large as that in the cluster separation stage. From the floral bud separation stage to the 100% blooming stage, the change in the diameter of the flowers was less than 0.1 mm, and the flower cap of the ovary was completely detached from the morphology. From the 100% blooming stage to fruit setting stage, the diameter of the flower ovary increased by 0.7 mm, the epidermal cells of the ovary expanded and the stigma began to collapse [Fig. 3](#).

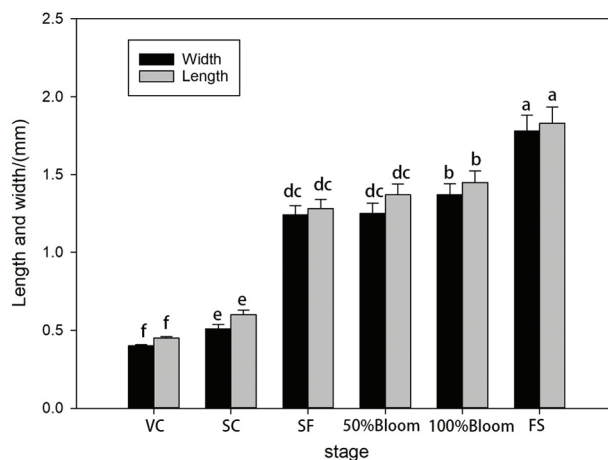


Figure 3: Statistics of ovary size of ‘Summer Black’ flower

3.3 Observations of the Formation and Anatomical Structures of Vascular Bundles in Grapevine Flowers (Ovaries)

After the sample had been clarified, the structure and composition of the flower’s vasculature could be easily identified. The vascular bundles of ‘Summer Black’ pedicels branched into the ovary to form the vascular bundles of the flower ovary (Fig. 4A), which could be divided into the peripheral vascular bundle, the central vascular bundle and the ovule vascular bundle according to the distribution (Figs. 4B and 4C). The peripheral vascular bundles were located in the lower layer of the ovary’s epidermal cells, and was composed of first-order vascular bundles and inferior vascular bundles. The first-order vascular bundles branched directly from the pedicel and met directly below the style, and the adjacent first-order vascular bundles were connected to the inferior vascular bundles of its branches. The inferior vascular bundles were not directly connected with the flower stalk but branched from the upper vascular bundles and connected with the adjacent vascular bundles to form a closed-loop vascular structure. The central vascular bundles consisted of two vascular bundles, which were located in the center of the ovary and connected the intersection of the pedicel and the junction of the first-order vascular bundles. The central vascular bundles branched into the ovule at the basal part of the embryo to form the ovule vascular bundle (Fig. 4).

The distance from the peripheral vascular bundles to the ovary epidermal cells changed obviously from the visible cluster stage to the fruit setting stage. The distance increased by nearly 4.5-fold, and followed a double sigmoid curve, in accordance with the changes in the size of the ovary. The growth from the visible cluster stage to the floral bud separation stage was strong, the growth from the floral bud separation stage to the 50% blooming stage was slower, and the growth from the 100% blooming stage to the fruit setting stage was strong (Fig. 4A).

3.4 Observations of Vascular Development around the Ovary of Grapevine Flowers

The data on the development of the vascular bundles of the flower ovary in each stage were obtained by observation after optical clearing of the tissues. During the visible cluster stage, the structure of the vascular bundles around the flower ovary was simple, with the length of the first-order vascular bundle being less than 500 μm (Fig. 6B). With only four branch points and four first-order vascular bundles, only four inferior vascular bundles and no low-level vascular bundles could be seen (Fig. 5A).

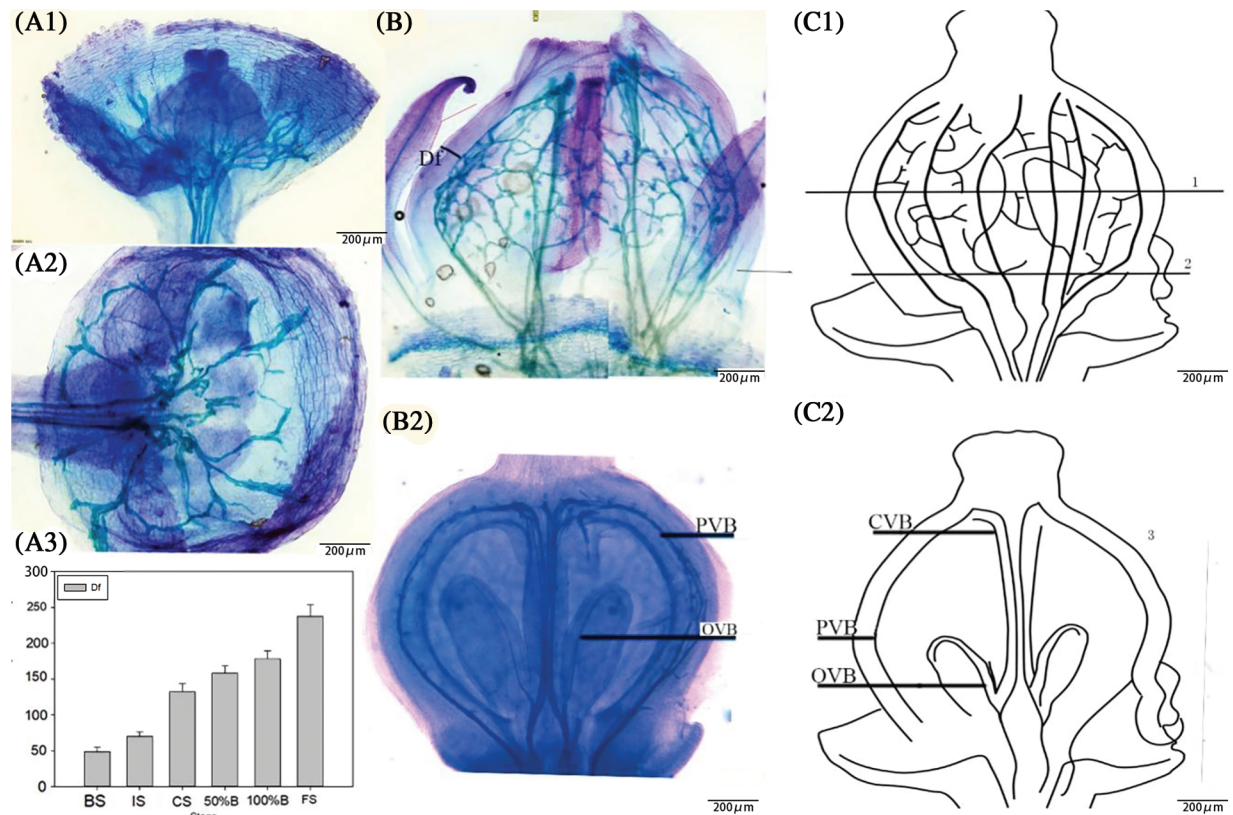


Figure 4: (A) Observation diagram of vascular formation of flower ovary. (A1) Flower stalk entered the ovary at the visible clusters stage and there were only three first-order vascular bundles. (A2) The formation of flower ovary vascular bundles. (A3) The distance from ovary to peripheral vascular bundles in each stage. (B) Observation diagram of vascular formation of flower ovary. (B1) Peripheral vascular bundles entered from fruit stalk and branch into first-order vascular bundles and inferior vascular bundles. Df Distance from peripheral vascular bundle to the epidemic cell; PVB Peripheral vascular bundle; OVB Ovary vascular bundle; (B2) The central vascular bundle entered from the fruit stalk, and branches from the ovule in the ovary. (C) Schematic diagram of vascular distribution. (C1) Peripheral vascular bundles enter from fruit stalk and branch into first-order vascular bundles and inferior vascular bundles. (C2) The central vascular bundles entered from the fruit stalk, and branch from the ovule in the ovary. CVB Central vascular bundle; PVB Peripheral vascular bundle; OVB Ovary vascular bundle

With the change in the development stage, the length of the first-order vascular bundle and the number of branch points increased (Fig. 5). The length of the first-order vascular bundles increased fivefold from the visible cluster stage to the fruit setting stage, and the number of branch points changed from 2 to more than 160 (Fig. 6A). The number of first-order vascular bundles changed from 4 to 12. The growth data showed a double sigmoid shape with a strong increase in diameter during the early stages (from the visible cluster stage to the floral bud separation stage), a slower phase (the length of the main vascular bundle increased little between the floral bud separation stage and the 50% blooming stage) and changed greatly from the 100% blooming stage to the fruit setting stage.

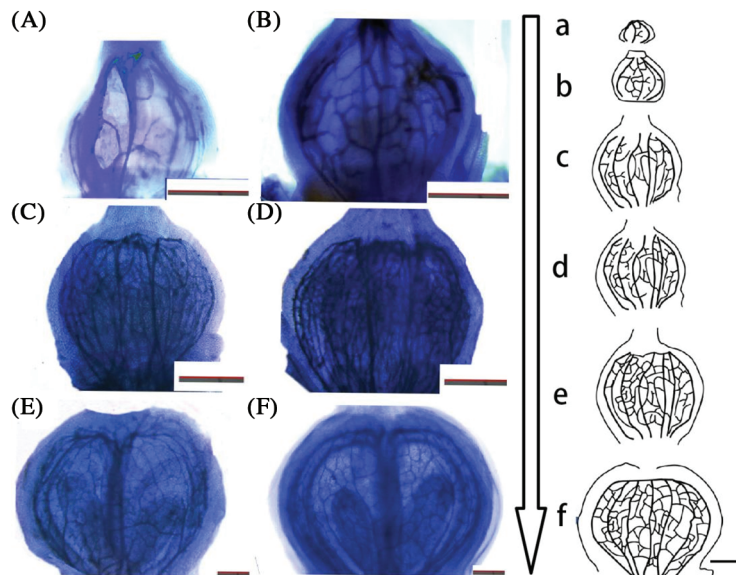


Figure 5: Ovary development pattern of ‘Summer Black’ flower. (A, a) visible clusters; (B, b) separated clusters; (C, c) separated floral buds; (D, d) 50% Bloom; (E, e) 100% Bloom; (F, f) fruit setting stage (scale 200 μm)

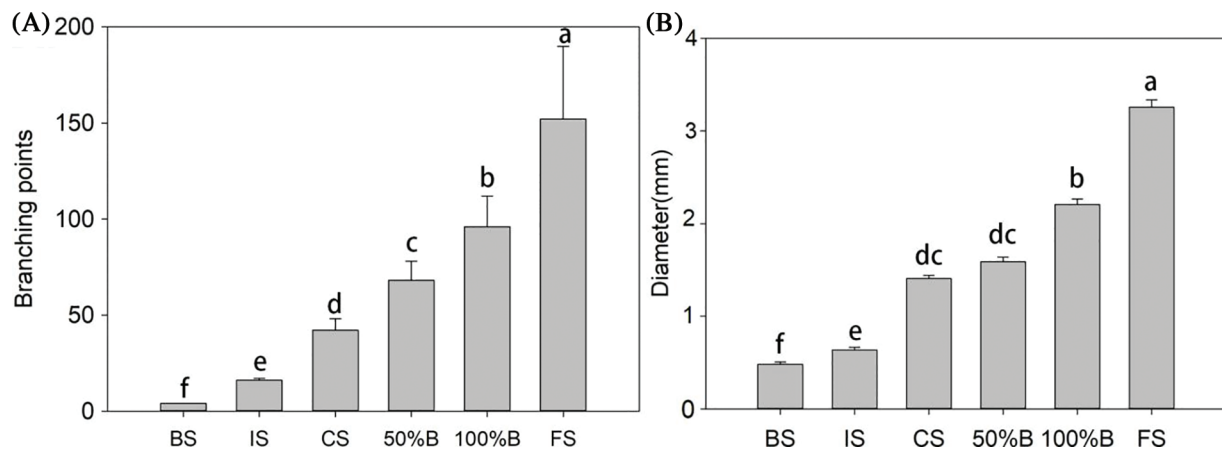


Figure 6: (A) number of branch points of peripheral vascular bundle; (B) length of first-order vascular bundle

3.5 Observations of the Structure and Size Development of the Vessels of Grapevine Ovaries

After the tissue had been treated, we could clearly see the vertical structure and details of the flower ovary’s vessels (Fig. 7). The changes in the vessels’ width and length were not the same in different developmental stages. The length of a single first-order vessel was less than 70 μm in the visible cluster period, and the length of a single first-order vessel doubled from the visible cluster stage to the floral bud separation stage. The average length of a single first-order vessel was more than 120 μm in the floral bud separation stage. During the floral bud separation stage, the average length of a single vessel was basically unchanged, and the average lengths of the first-order and second-order vessels increased by 36.42 and 37.68 μm , respectively, from 100% blooming to the fruit setting stage (Fig. 8). The second-order vessels were thinner and shorter than the first-order vessels in the same period, but the overall trend

of the changes in length were consistent. As a result, the change trend of the length of a single vessel was consistent with the change trend of the size of the ovary.

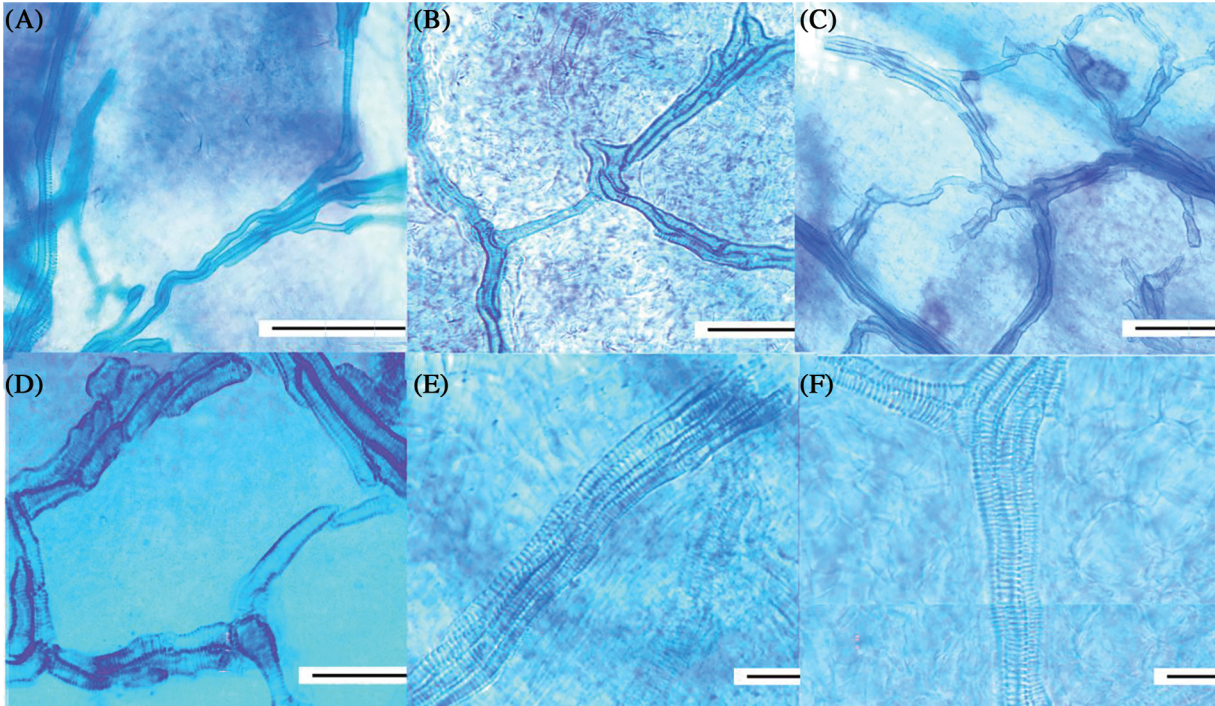


Figure 7: Flower ovary vessels in different periods by tissue clear. (A) showed that the vessels structure was simple, the number of single vessels was small, and the thread was not obvious; (B) There were several branch threads in vascular bundle, and the vascular bundle was composed of multiple vessels; (C) thread was obvious, the number of vessels increased; (D) vascular bundle branching points obviously increased; (E) the vessels were longer and thicker, and the perforated plate of dimensional tube thread is clear; (F) the fruit-set having largest length and width (scale 100 μm). (A–F) The vast majority of vessels was helical almost all stage

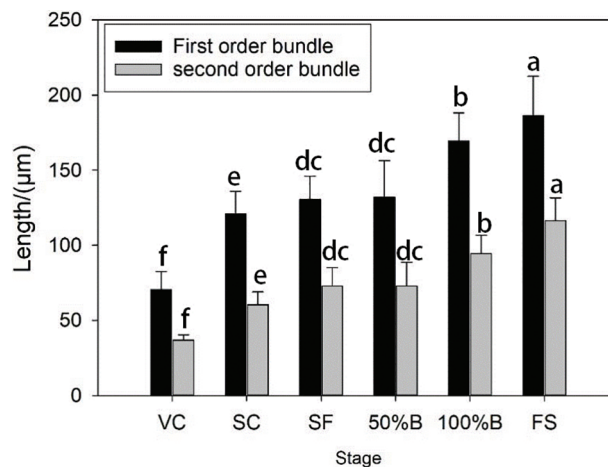


Figure 8: Changes of length and width of first-order vessel and secondary vessel of ovary in grape flower

3.6 Observations of Vascular Branches and the Three-Dimensional Arrangement around the Ovary of Grape Flowers

Because the optical clearing technique did not damage the overall structure of the vascular network of the ovary, the fluorescence was bright and the field of vision was clear under the fluorescence microscope. The vasculature of the grape ovary was suitable for three-dimensional imaging by confocal microscopy. The three-dimensional observations obtained by confocal imaging showed that the peripheral vascular bundles at different branch levels were not all on the same plane (Fig. 9). Near the area of the stigma, the reflux structure formed by the horizontally connections at all levels of the vascular bundle was not in the same plane as the vertical vascular bundle (Fig. 9A). The superior and inferior vascular bundles in the middle of the ovary's vascular bundles were not in the same plane (Fig. 9B).

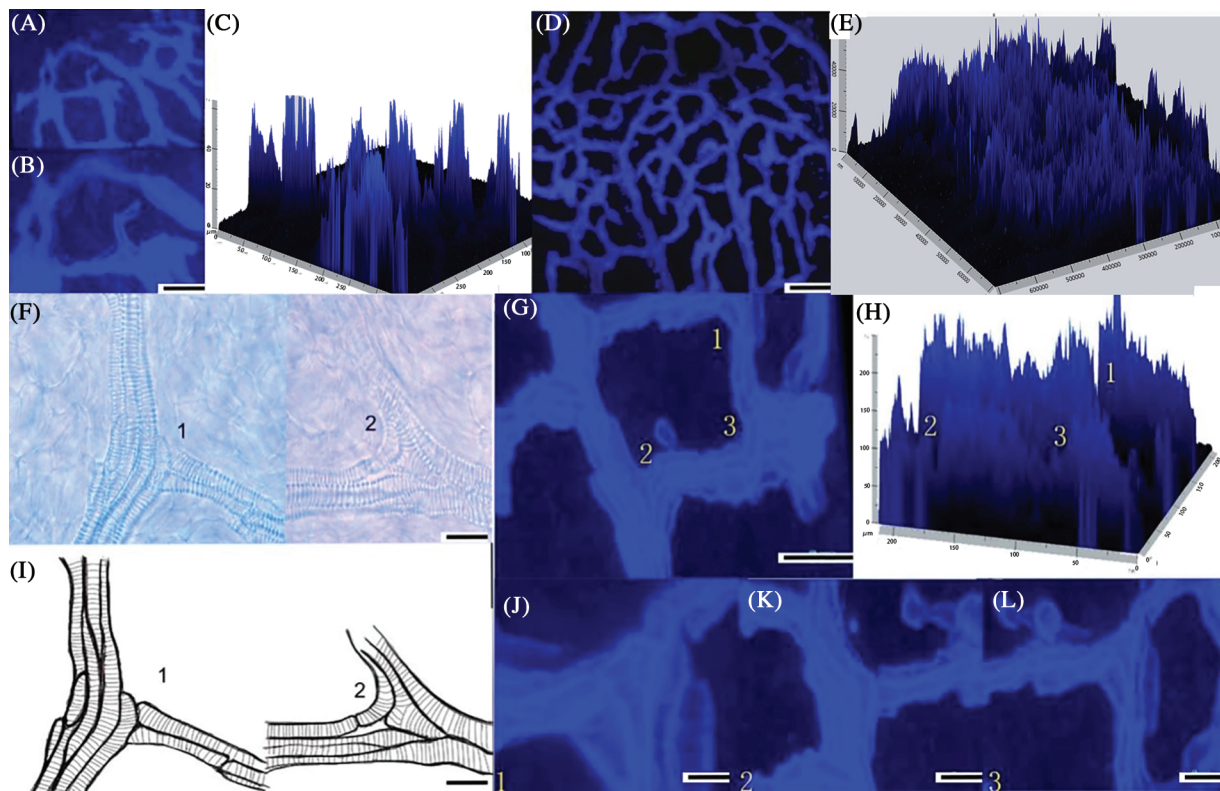


Figure 9: (A, B) The transverse vascular bundles and vertical vascular in stigma area were not in the same plane by confocal scanning; (C) 3-D image of the transverse vascular bundles and the vertical vascular bundles and the height could be measured; (D) The vascular bundles inside the ovary were uneven; (E) The 3-D image of vascular bundles inside the ovary and the height could be measured; (F) 1. The lower vascular was directly connected with the upper vascular; 2. Vascular connect through the metamorphosis of the three-way; Mv, Metamorphic vessel; (G) 1, 2, 3 (J, K, L) There was a height difference between the main veins and branch veins connected by different ways ; (H) The 3-D image of vascular bundles with different patterns have difference in height (scale 50 μm); (C, E, H) The height of the vascular bundles viewed in pictures represent the relative height of each vessel in vasculature

The patterns of the vascular bundles may be one of the reasons why they were not in the same plane. However, vascular bundles branch in three directions (transversal, oblique and longitudinal) with no random patterns. According to the 3D reconstruction, we can summarize these vascular bundles branches

in two different ways. First, the superior vascular bundles attached parallel to the first inferior vessels (Figs. 9A and 9B). Secondly, some bent in different ways, forming the inferior vascular bundles (Fig. 9C). The vessels that eventually developed were very different from the other vessels. The shapes of the ending vein vessels were irregular and varied. Different attachment methods made the vascular have different intercepts. The occurrence and continuous arrangement of these two branching patterns led to an uneven vasculature.

3.7 Observations and Comparisons of Paraffin Sectioning

3.7.1 Observation and Comparison of the Structure of the Vascular Bundle Obtained via Paraffin Sectioning

The structural diagram obtained by paraffin sectioning (the position of the section can be seen in Fig. 4) showed the same results as the first experiment, but compared with the method of observing the vascular branching described in this study, the longitudinal distribution could be observed. It was difficult to distinguish the ovary's vascular bundle from the central vascular bundle (Fig. 10).

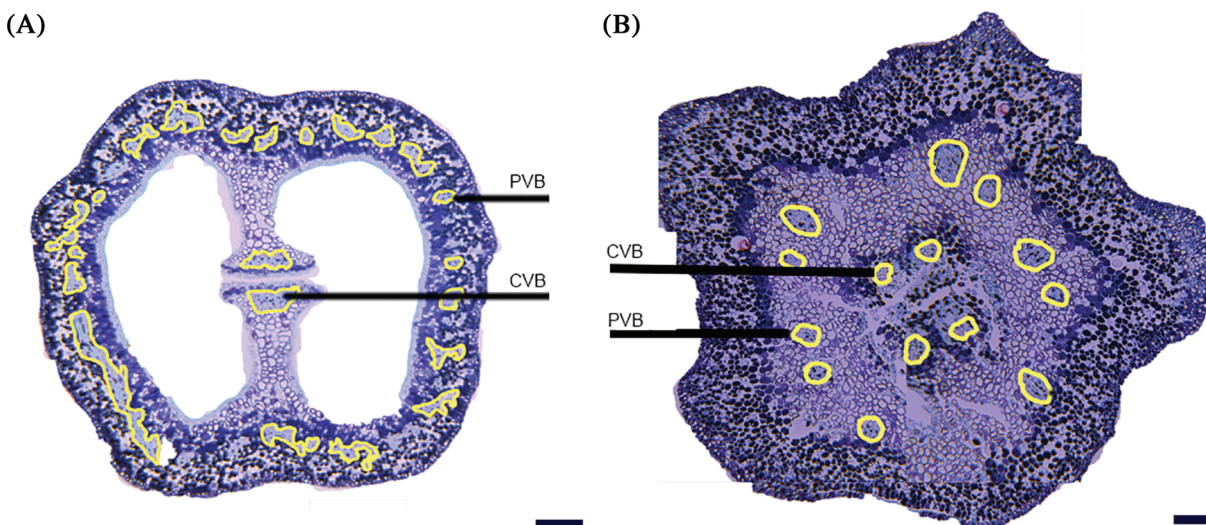


Figure 10: Flower ovary vascular section; (A) the peripheral vascular bundle was distributed in the lower volume of ovary epidemic cell, and the central vascular bundle consists of two parts in separated floral bud stage; (B) paraffin section showed the number and distribution of peripheral vascular bundle, and it was difficult to distinguish the central vascular from the ovary vascular bundle (scale 50 μm). PVB peripheral vascular bundle; OVB ovary vascular bundle; CVB central vascular bundle

3.7.2 Observation and Comparison of the Size of the Vascular Bundle Obtained via Paraffin Sectioning

When we observed the vascular bundles of ovary by paraffin sectioning, it was difficult to identify the position of the vertical section because the vascular bundles around the ovary were not in the same plane. Cross-cutting of ovary can allow observations of only the size and composition of the vascular bundles. The first-order vascular bundle in the visible cluster stage consists of only four vessels, and the first-order vascular bundle in the fruit setting stage consisted of up to 84 vessels (Fig. 11).

3.8 Summary of the Vascular Development of Grape Ovaries

By observing the vascular development of the grape ovary in different periods after optical clearing of the tissues, the anatomical results indicated that, firstly, the vasculature of the flowers was formed by the vascular bundles of the pedicel entering the ovary and branching. Its anatomical structure was consistent with the vascular structure of the fruit, and the vascular bundles of the fruit were formed by the vascular bundles of the ovary. Secondly, the first-order vascular bundles around the flower increased from the

visible cluster period to the floral bud separation stage, from four first-order vascular bundles to 12 first-order vascular bundles. Third, during development, the floral vasculature branched in three directions (transversal, oblique, and longitudinal) in two ways. Firstly, the superior vascular bundles attached parallel to the first inferior vascular bundles; secondly, some bent in different ways, forming the inferior vascular bundles (Fig. 9C). The vessels that eventually developed were very different from the other vessels. The shapes of the ending vein vessels were irregular and varied. Different attachments methods made the vascular have different intercepts. Lastly, the vasculature of the flower ovary developed continuously during the development of the ovary to adapt to the changes.

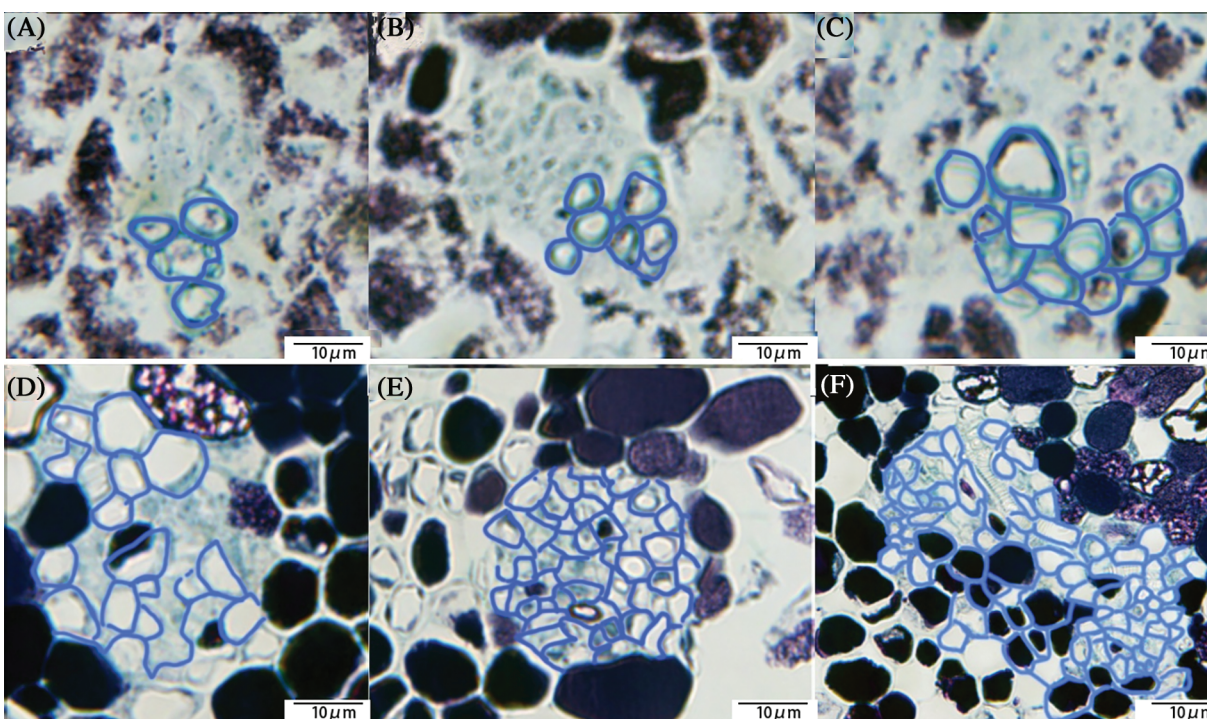


Figure 11: Ovary vascular section; (A) Paraffin section showed the vascular section at the visible cluster stage, with only four vessels in a single vascular bundle; (B) The number of vascular bundles in a single vascular bundle increased at the separated floral buds, and the transverse diameter of vascular bundles increased greatly; (C) The single vascular consisted of more than 10 vessels; (D) The difference between the separated floral buds stage and the 50% bloom stage was small; (E) The size and number of vessels in the 100% bloom stage started to increase again; (F) The vascular in the fruit setting stage (scale 10 μm)

4 Discussion

4.1 Advantages of the Optical Clearing Technique for Observing the Vascular Development of the Grape Ovary

The discovery and use of the optical clearing technology can be traced back to the last century. Thanks to the development of optics and the continuous discovery of chemical optical clearing agents, this technology has been widely used in the biological sciences in recent years [21,22]. In 2013, the optical clearing technique was rated as one of the top 10 scientific breakthroughs in medical research [23]. As a revival technology, the optical clearing method has the advantage of adapting to 3D reconstructions and computer sample analyses based on cell resolution algorithms [24]. It has also been taken advantage of in botanical research for some

tiny plant tissues with poor slicing ability. The optical clearing method can quickly allow us to observe the internal structure and development process of tissues.

4.2 Relationship between the Ovary's Vasculature and the Fruit's Vasculature

The anatomical structure of the ovary's vascular bundles was similar to that of the fruit, and the vascular bundles of the pedicel immediately branched into peripheral vascular bundles, central vascular bundles and ovule vascular bundles after entering the flower ovary. This indicated that the fruit's vascular bundles were formed in the flower ovary's vascular bundles, consistent with the conclusions of Pratt and Galet [25,26].

4.3 Vascular Differentiation of the Ovary Followed a Sequence

In the development of dicotyledonous angiosperm leaves, the vascular system can be observed to form gradually and sequentially. This increase in the complexity of the vascular network by the addition of vascular bundles was also observed in the development of dicotyledonous angiosperm plants. During leaf elongation, the vasculature was laid down progressively and sequentially. The procambial bundles of the first-order and secondary veins are laid down first, followed by the progressive acropetal and basipetal differentiation of vessels [27]. As the leaf lamina expands, the areoles formed by tertiary veins are subdivided by the veins of the next order, and this process is reiterated by higher-order minor veins until the leaf is mature and stops expanding. In the development of dicotyledonous angiosperm leaves, the vasculature can be observed to form gradually and sequentially [28]. However, no similar situation was found in the anatomy of the vascular development of fruit [9,10]. Chatelet speculated that in the early stages of vascular development in fruit, the vascular bundle was composed of one single vascular bundle connecting the pedicel to the vascular top place under the style [10]. In this study, it was found, for the first time by this experimental method, that the number of first-order vascular bundles of grapevine flowers in the visible cluster stage was less than that in the subsequent stage, which means the first-order vascular bundles around the flowers differentiated in a sequence.

4.4 Patterns and Directions of the Vascular Branches of the Ovary

The branching direction of the flower's vascular system is very complicated during the development period [9,10]. Aloni believed that floral development follows the ABC box theory. The direction of branching of vascular bundles is related to the auxin concentration gradient [29–31]. This experiment found that the branching patterns of the vascular bundles of flowers also affected the direction of the vascular branches of the flower organs in three dimensions. These two branching patterns have been mentioned many times in studies on the vascular development of leaves [27,31–33]. These two patterns are considered to have effects on the hydraulics and mechanical support, but their functions, significance and mechanism of production still need to be investigated [34,35].

The secondary cell wall patterns of ovary vessels were almost all helical, with few annular examples found in our research. This result is consistent with secondary cell wall patterns of grape vessels which were studied by Chatelet [10]. Helical secondary cell walls could allow an increase in the distance between rings in older xylem elements for easier longitudinal stretching. Due to the continuous expansion of the ovary during its development, the helical shape is economic and useful for the expansion in the distance of the helical wall thickenings of the protoxylem [36]. Another reason why the ovary vessels were almost all helical and few were annular is that the ovary is a flesh organ of the grapevine which had less time for the patterns to become pitted or reticulated, patterns which have been reported to develop from helical and annular patterns after a longer time [37,38].

4.5 Size and Position of the Ovary's Vascular Bundles and Vessels

The distance from the peripheral vascular bundles around the ovary to the epidermal cells gradually increased, which was basically the same as the development trend of flower size. The size of single first-order peripheral vascular bundles was consistent with the increasing trend of ovary size. This is because the change in the vascular size comes from the adaptation of the vasculature to the development of floral organs through stretching, the differentiation of new vascular bundles and the differentiation of the vessel molecules in the vascular bundles [7,35].

The number of vascular branch points increased during all the developmental periods of the flowers, which meant that the vascular bundles remained differentiated from the floral bud separation stage to the 50% blooming stage, when there was little change in the vascular size of the flowers. It is believed that the differences in the auxin concentration gradient lead to the proliferation and differentiation of vascular bundles. There is no relevant report on how this mechanism leads to the increase in branching points and the small change in the average vascular size of flower organs during the period from the floral bud separation stage to the 50% blooming stage. Grapevine is a special kind of closed-pollinated plant, and the reason why the vascular size changes little in this period may be related to this [39,40]. The grapevine flower experiences a major morphological change from the floral bud separation stage to the 50% blooming stage [1]. Koussa reported that the total ABA content in flower organs increased significantly at this stage and reached the maximum at flowering stage, and then the ABA content began to decrease [41]. A large amount of ABA not only promotes the shedding of the flower cap but may also inhibit the development of the flower's vascular system [42,43].

5 Conclusion

Above all, the optical clearing method can allow the growth, development and structure of the vascular system of grapevine flowers to be systematically and completely observed and studied. The development trends of the vascular growth dynamics of 'Summer Black' flower ovaries observed via paraffin sectioning and optical clearing were compared. It was found that the observations after optical clearing had advantages over paraffin sectioning. The laser confocal and three-dimensional reconstruction techniques were successfully used to explore the peripheral vascular structure of 'Summer Black' flower ovaries. The optical clearing technique had advantages for observing tiny tissues and organs, and it is feasible to apply this technique in the study of grapevine flowers.

Funding Statement: This work was supported by the Grants 31872050 from the National Natural Science Foundation of China.

Author Contributions: Zhaosen Xie conceived the idea and supervised the work, Teng Fei performed experiments and analysed data, and Teng Fei, Youmei Li and Bo Li wrote and revised the manuscript.

Conflicts of Interest: The authors declare that they have no conflicts of interest to report regarding the present study.

References

1. Lorenza, D. C., Mickael, M., Ivana, G. (2017). Breeding next generation tree fruits: Technical and legal challenges. *Horticulture Research*, 4, 17067.
2. Ma, X. Y., Jiao, W. Q., Li, H., Zhang, W., Ren, W. C. et al. (2022). Neopetalotriopsis eucalypti, a causal agent of grapevine shoot rot in cutting nurseries in China. *Journal of Integrative Agriculture*, 8, 3684–3691.
3. Keller, M. (2017). *The science of grapevines*. USA: Academic Press.
4. Holzapfel, B., Clcbment, C., Vaillant-Gaveau, N., Wojnarowicz, G., Lebon, G. et al. (2008). Sugars and flowering in the grapevine (*Vitis vinifera* L.). *Journal of Experimental Botany*, 59(10), 2565–2578.

5. Zheng, W., García, J., Balda, P., de Toda, F. M. (2017). Effects of late winter pruning at different phenological stages on vine yield components and berry composition in La Rioja, North-Central Spain. *Journal International des Sciences de la Vigne et du Vin*, 51(4), 363–372.
6. Bondada, B. R., Matthews, M. A., Shackel, K. A. (2005). Functional xylem in the post-veraison grape berry. *Journal of Experimental Botany*, 56(421), 2949–2957.
7. Castelan-Estrada, P., Gaudillere, J. P. (2002). Allometric relationships to estimate seasonal above ground vegetative and reproductive biomass in *Vitis vinifera*. *Annals of Botany*, 89, 401–408.
8. Yanina, G., Pugliese, B., Gonzalez, C. (2021). Spray with plant growth regulators at full bloom may improve quality for storage of ‘Superior Seedless’ table grapes by modifying the vascular system of the bunch. *Postharvest Biology & Technology*, 176, 111522.
9. Chatelet, D. S., Matthews, M. A., Rost, T. L., Shackel, K. A. (2008). The peripheral xylem of grapevine (*Vitis vinifera*). 1. Structural integrity in post-veraison berries. *Journal of Experimental Botany*, 59(8), 1987–1996.
10. Chatelet, D. S., Matthews, M. A., Rost, T. L., Shackel, K. A. (2008). The peripheral xylem of grapevine (*Vitis vinifera*) berries. 2. Anatomy and development. *Journal of Experimental Botany*, 59(8), 1997–2007.
11. Yimi, B., Mun, J. H., Jeong, Y. M., Hur, Y. Y., Yu, H. J. (2015). Flower and microspore development in ‘Campbell Early’ (*Vitis labruscana*) and ‘Tamnara’ (*V. spp.*) grapes. *Korean Journal of Horticultural Science and Technology*, 33(3), 141–148.
12. Bondada, B. R., Mark, M. A., Kenneth, S. A. (2005). Functional xylem in the post-veraison grape berry. *Journal of Experimental Botany*, 56(421), 2949–2957. <https://doi.org/10.1093/jxb/eri291>
13. Keller, M., Jason, P. S., Bondada, B. R. (2006). Ripening grape berries remain hydraulically connected to the shoot. *Journal of Experimental Botany*, 57(11), 2577–2587. <https://doi.org/10.1093/jxb/erl020>
14. Silvestroni, O., Lanari, V., Lattanzi, T., Palliotti, A. (2019). Canopy management strategies to control yield and grape composition of Montepulciano grapevines. *Australian Journal of Grape and Wine Research*, 25(1), 30–42. <https://doi.org/10.1111/ajgw.12367>
15. Knipfer, T., Fei, J., Gambetta, G. A., McElrone, A. J., Shackel, K. A. et al. (2015). Water transport properties of the grape pedicel during fruit development: Insights into xylem anatomy and function using microtomography. *Plant Physiology*, 168(4), 590–1602. <https://doi.org/10.1104/pp.15.00031>
16. Xiao, Z., Gardner, T. S., Willis, S. A., Price, W. S., Moroni, F. J. et al. (2021). 3D visualisation of voids in grapevine flowers and berries using X-ray micro computed tomography. *Australian Journal of Grape and Wine Research*, 27(2), 141–148. <https://doi.org/10.1111/ajgw.12480>
17. Zhao, H. (2020). 3D imaging of cleared tissues. *The FASEB Journal*, 34(1), 1.
18. Lebon, G., Duchêne, E., Brun, O., Clément, C. (2005). Phenology of flowering and starch accumulation in grape (*Vitis vinifera* L.) cuttings and vines. *Annals of Botany*, 95(6), 943–948.
19. Xie, Z. S., Guo, X. J., Cao, H. M. (2013). Effect of root restriction on vegetative growth and leaf anatomy of ‘Kyoho’ grapevines cultivar. *African Journal of Agricultural Research*, 8(15), 1304–1309.
20. Xie, Z. S., Forney, C. F., Cao, H. M., Bo, L. (2014). Changes in water translocation in the vascular tissue of grape during fruit development. *Pakistan Journal of Botany*, 46(2), 483–488.
21. Richardson, D. S., Guan, W., Matsumoto, K., Pan, C., Chung, K. et al. (2013). Tissue clearing. *Nature Reviews Methods Primers*, 1(1), 84.
22. Kanatani, S., Uhlén, P. (2022). Imaging cleared tissues made easy. *Nature Methods*, 19(5), 527–529. <https://doi.org/10.1038/s41592-022-01424-3>
23. Liu, Y. A., Chung, Y. C., Pan, S. T., Shen, M. Y., Hou, Y. C. et al. (2013). 3-D imaging, illustration, and quantitation of enteric glial network in transparent human colon mucosa. *Neurogastroenterology and Motility*, 25(5), 324–338. <https://doi.org/10.1111/nmo.12115>
24. Wei, Z. M., Lin, Q. Y., Lazareva, E. N., Dyachenko, P. A., Yang, J. et al. (2021). Optical clearing of laser-induced tissue plasma. *Laser Physics Letters*, 18(8), 424–435. <https://doi.org/10.1088/1612-202X/ac0e40>
25. Pratt, C. (1974). Vegetative anatomy of cultivated grapes—A review. *American Journal of Enology and Viticulture*, 22(3), 92–109. <https://doi.org/10.5344/ajev.1974.25.3.131>

26. Galet, P. (2002). *General viticulture*. France: Oenopluri Media and P.Galet.
27. Chatelet, D. S., Matthews, M. A., Rost, T. L. (2006). Xylem structure and connectivity in grapevine (*Vitis vinifera*) shoots provides a passive mechanism for the spread of bacteria in grape plants. *Annals of Botany*, 98(3), 483–494. <https://doi.org/10.1093/aob/mcl124>
28. Aloni, R. (2021). *Vascular differentiation and plant hormones*. Switzerland: Springer Nature Switzerland AG.
29. Aloni, R., Schwalm, K., Langhans, M., Cornelia, I. U. (2003). Gradual shifts in sites of free-auxin production during leaf-primordium development and their role in vascular differentiation and leaf morphogenesis in Arabidopsis. *Planta*, 216(5), 841–853.
30. Sachs, T. (1981). The control of the patterned differentiation of vascular tissues. *Advances in Botanical Research*, 9, 151–262.
31. Merrill, E. K. (1979). Comparison of ontogeny of three types of leaf architecture in *Sorbus* L. *Botanical Gazette*, 140, 328–337.
32. Fisher, D. G. (1985). Morphology and anatomy of the leaf of coleus blumei (*Lamiaceae*). *American Journal of Botany*, 72(3), 392–406.
33. Fisher, D. G., Evert, R. F. (1982). Studies on the leaf of amaranthus retroflexus (*Amaranthaceae*): Morphology and Anatomy. *American Journal of Botany*, 69(7), 1133–1147.
34. Li, Y. M., Teng, F., Zhang, H. X., Xie, Z. S., Bo, L. (2023). Observation of the development of leaf vein and stomata and identification candidate transcription factors related to vein/stoma development in grapevine leaf (*Vitis vinifera* L.). *Scientia Horticulturae*, 307, 111518.
35. Thorne, E. T., Young, B. M., Young, G. M., Stevenson, J. F., Labavitch, J. M. et al. (2006). The structure of xylem vessels in grapevine and a possible passive mechanism for the systemic spread of bacterial disease. *American Journal of Botany*, 93, 497–504.
36. MacAdam, J. W., Nelson, C. J. (2002). Secondary cell wall deposition causes radial growth of fibre cells in the maturation zone of elongating tall fescue leaf blades. *Annals of Botany*, 89, 89–96.
37. Xu, H. Z., Giannetti, A., Sugiyama, Y., Zheng, W. N., Schneider, R. et al. (2022). Secondary cell wall patterning—Connecting the dots, pits and helices. *Open Biology*, 12(5), 210208.
38. Yamaguchi, M., Mitsuda, N., Ohtani, M., Ohme-Takagi, M., Kato, K. et al. (2011). Vascular-related nac-domain 7 directly regulates the expression of a broad range of genes for xylem vessel formation. *Plant Journal*, 66, 579–590.
39. Filippetti, I., Silvestroni, O., Thomas, M. R., Intrieri, C. (1999). Diversity assessment of seedlings from self-pollinated Sangiovese grapevines by ampelography and microsatellite DNA analysis. *VITIS*, 38(2), 67–71.
40. Filippetti, I., Silvestroni, O., Thomas, M. R., Intrieri, C. (2000). Diversity assessment of seedlings from self-pollinated ‘sangiovese’ grapevines (*Vitis vinifera* L.) by ampelography and microsatellite dna analysis. *Acta Horticulturae*, 528, 147–154.
41. Koussa, T., Colin, L., Broquedis, M. (2004). Endogenous levels of abscisic acid in various organs of *Vitis vinifera* L. (cv. Cabernet Sauvignon) between flower bud separation and grape closing stages. *Journal International des Sciences de la Vigne et du Vin*, 38(2), 141–146.
42. Ramachandran, P., Wang, G. D., Augstein, F., Annelie, J. D., Carlsbecker, A. (2018). Continuous root xylem formation and vascular acclimation to water deficit involves endodermal ABA signalling via miR165. *Development*, 145(3), 195–202.
43. Rancic, D., Quarrie, S. P., Dodd, I. (2007). Transport of growth regulators to developing xylem tissues: Plant ABA status impacts on hydraulic conductance by modifying xylem vessel development. *Comparative Biochemistry and Physiology*, 146(4), S235–S242.